The Recycling and Transcytotic Pathways for IgG Transport by FcRn are Distinct and Display an Inherent Polarity

The recycling and transcytotic pathways for IgG transport by FcRn are distinct and display an inherent polarity

Salit Tzaban,[1] Ramiro H. Massol,[1] Elizabeth Yen,[1] Wendy Hamman,[1] Scott R. Frank,[1] Lynne A. Lapierre,[4,5] Steen H. Hansen,[1] James R. Goldenring,[4,5] Richard S. Blumberg,[2,3] and Wayne I. Lencer[1,3]

[1]Children's Hospital, Gastroenterology Division; [2]Brigham and Women's Hospital, Gastroenterology Division; and the [3]Harvard Digestive Diseases Center, Harvard Medical School, Boston, MA 02115
[4]Deptartment of Surgery, Epithelial Biology Center, Vanderbilt University School of Medicine, Nashville, TN 37232
[5]Nashville Veterans Affairs Medical Center, Nashville, TN 37232

The Fc receptor FcRn traffics immunoglobulin G (IgG) in both directions across polarized epithelial cells that line mucosal surfaces, contributing to host defense. We show that FcRn traffics IgG from either apical or basolateral membranes into the recycling endosome (RE), after which the actin motor myosin Vb and the GTPase Rab25 regulate a sorting step that specifies transcytosis without affecting recycling. Another regulatory component of the RE, Rab11a, is dispensable for transcytosis, but regulates recycling to the basolateral membrane only. None of these proteins affect FcRn trafficking away from lysosomes. Thus, FcRn transcytotic and recycling sorting steps are distinct. These results are consistent with a single structurally and functionally heterogeneous RE compartment that traffics FcRn to both cell surfaces while discriminating between recycling and transcytosis pathways polarized in their direction of transport.

Introduction

The major histocompatibility complex class I–related receptor FcRn traffics IgG across polarized epithelial cells that line mucosal surfaces, affecting immune surveillance and host defense (Bitonti et al., 2004; Yoshida et al., 2004, 2006). Unlike the polymeric Ig receptor (pIgR) that mediates the polarized secretion of dimeric IgA (dIgA), FcRn moves IgG in both directions across epithelial barriers to provide a dynamic exchange between circulating and lumenal IgG at mucosal sites (Dickinson et al., 1999; Claypool et al., 2002, 2004). Uniquely, FcRn is one of the few proteins to move inward from the apical to basolateral membrane by transcytosis, a pathway poorly understood but highly significant for the absorption of environmental antigens and microbial products. Another hallmark of FcRn function is that the receptor sorts IgG away from lysosomes, explaining why IgG has the longest half-life of any circulating serum protein and allowing for the development of durable protein therapeutics that interact with the receptor (Ghetie et al., 1996; Israel et al., 1996; Junghans and Anderson, 1996; Bitonti et al., 2004; Dumont et al., 2005; Wani et al., 2006; Mezo et al., 2008). How FcRn sorts IgG between apical and basolateral cell surfaces of epithelial cells to accomplish these functions remains poorly understood.

FcRn is a heterodimer composed of a glycosylated heavy chain associated with β2-microglobulin. Binding of IgG to FcRn requires contact between the Fc domain of IgG and the extracellular heavy chain of FcRn (Burmeister et al., 1994; Medesan et al., 1998). Unlike the other Fcγ receptors, FcRn shows high-affinity binding for IgG only at an acidic pH (Rodewald, 1976; Raghavan et al., 1993).

The pathway for transcytosis across polarized epithelial cells is best understood for pIgR (Apodaca et al., 1994; Rojas and Apodaca, 2002). pIgR binds dIgA on the basolateral membrane and carries it sequentially into the early basolateral endosome, the recycling endosome (RE; sometimes termed the common RE in polarized cells), and finally to the apical cell surface, where the

Correspondence to Wayne I. Lencer: wayne.lencer@childrens.harvard.edu

Abbreviations used in this paper: ANOVA, analysis of variance; ARE, apical recycling endosome; dIgA, dimeric IgA; MyoVb, myosin Vb; NIP, 4-hydroxy-3-iodo-5-nitrophenylacetyl; pIgR, polymeric Ig receptor; RE, recycling endosome; shRNA, small hairpin RNA; TetR, tetracycline repressor; Tf, transferrin; Tf-R, Tf receptor.

The Rockefeller University Press $30.00
J. Cell Biol. Vol. 185 No. 4 673–684
www.jcb.org/cgi/doi/10.1083/jcb.200809122

receptor is cleaved for release into the lumen as secretory IgA. The RE is an operationally defined sorting compartment (for reviews see Hoekstra et al., 2004; Maxfield and McGraw, 2004; van Ijzendoorn, 2006) that harbors the bulk of FcRn in nonpolarized cells (Ward et al., 2005). In nonpolarized cells, the RE is a major site for recycling of apo-transferrin (Tf) by the Tf receptor (Tf-R), and this is dependent on the small GTPase Rab11a (Ullrich et al., 1996). In polarized epithelial cells, the RE defines a common site for recycling ligands internalized via the apical and basolateral membranes (Odorizzi et al., 1996; Wang et al., 2000b) and for transcytosis of dIgA by pIgR (Casanova et al., 1999; Sheff et al., 1999; Thompson et al., 2007).

Transcytosis of dIgA by pIgR from the basolateral membrane to the apical membrane requires sorting steps regulated by the small GTPases Rab11 and Rab25, and on the actin-based motor myosin Vb (MyoVb); but these proteins, including Rab11a, are not required for recycling Tf from the RE back to the basolateral membrane (Casanova et al., 1999; Wang et al., 2000b). This led to the concept of a separate endosomal compartment in polarized cells termed the apical RE (ARE), which is typified by the trafficking of protein and lipid cargoes to and from the apical membrane, but excluding vesicular traffic to the basolateral membrane (Apodaca et al., 1994; Casanova et al., 1999; Wang et al., 2000b; Lapierre and Goldenring, 2005; for review see van Ijzendoorn and Hoekstra, 1999). The physiological significance of the apical recycling pathway is emphasized by its role in regulating cell and tissue function (Forte et al., 1990; Casanova et al., 1999; Wang et al., 2000b; Tajika et al., 2004; Swiatecka-Urban et al., 2007), and in the biogenesis and maintenance of the apical membrane in intestinal cells (Muller et al., 2008) and hepatocytes (Wakabayashi et al., 2005). Still, the existence of such a compartment dedicated to apical membrane traffic remains unclear, and the results of most studies on this pathway are also consistent with apically directed sorting emanating from structurally heterogeneous and functionally distinct domains of the RE (Sheff et al., 1999; Wang et al., 2000a; van Ijzendoorn, 2006).

Here, we study what defines the polarity of transport for FcRn across polarized epithelial cells. Because the ARE components MyoVb, Rab11a, and Rab25 appear to regulate trafficking toward the apical membrane only, FcRn–IgG complexes moving across the cell in the reverse direction would be predicted to avoid these sorting steps, thus establishing polarity for basolaterally directed transport in a bidirectional pathway. Our results show, however, that MyoVb and Rab25 regulate a sorting step that is rate-limiting and specific to transcytosis in both directions without affecting the recycling pathways. This is not consistent with a separate endosomal compartment restricted to trafficking with the apical membrane. Rather, our data provide evidence for a single structurally and functionally heterogeneous RE that functions to sort FcRn among distinct recycling and transcytotic pathways, both differentiating between transport to apical and basolateral cell surfaces.

Results

We prepared MDCK cells stably coexpressing the human β_2m and the FcRn heavy chain fused at the N terminus to the hemaglutinin epitope HA, with or without EGFP at the C terminus. All cell lines also contained the tetracycline-dependent cis repressor. To assess FcRn function in IgG transport, we used a recombinant IgG against the hapten 4-hydroxy-3-iodo-5-nitrophenylacetyl (NIP) as a ligand (NIP-IgG; Claypool et al., 2004; Dickinson et al., 2008). To confirm specificity for FcRn, we used a mutant IgG containing inactivating mutations in the FcRn-binding site (NIP-IgG-IHH; Spiekermann et al., 2002). In this assay, NIP-IgG was applied to either surface of MDCK monolayers at 37°C, and transepithelial transport was measured in the contralateral reservoir by NIP-specific ELISA. Because low levels of FcRn-EGFP are expressed at the cell surface, this assay allows for pulse chase studies only after initially loading cells with IgG at 37°C, which is consistent with our previous studies using wild-type FcRn (Claypool et al., 2004) and with what has been recently documented in endothelial cells (Goebl et al., 2008).

MDCK cells expressing the fusion protein FcRn-EGFP transported IgG but not the mutant IgG-IHH in both directions across the monolayer (Fig. 1 a). Trafficking by FcRn was confirmed morphologically using Alexa Fluor 647–labeled Igs. Only wild-type IgG was taken up by the cells from either cell surface (Fig. 1 b), and this fraction was closely associated with FcRn-EGFP, as assessed by immunofluorescence, and quantified (Fig. 1 c; see Materials and methods and the immediately following paragraph, mean $M_{\text{target protein}} = 0.95$ and 0.98). We quantified compartments occupied by both proteins in 3D at steady-state by first identifying FcRn-EGFP– and IgG-containing objects using an automatic threshold-finding algorithm (Volocity, see Materials and methods; Costes et al., 2004), then analyzing the colocalization between FcRn-EGFP and IgG using the Manders colocalization coefficient (termed $M_{\text{target protein}}$). The Manders coefficient measures the strength of colocalization on a scale from 0 to 1, with 0 indicating no colocalizing signals and 1 indicating perfect colocalization. The distribution of Manders coefficients for each object is displayed as a scatter plot using 3D data obtained from multiple cells and independent experiments as indicated. All further colocalization studies were performed using the same method. In cells fixed at steady-state or imaged live over time, FcRn-EGFP and the lysosomal markers LAMP1 (Fig. 1 f and Video 1) or Lysotracker (not depicted) occupied almost completely different structures (mean $M_{\text{target protein}} = 0.02$). Thus, the C-terminal fusion of EGFP to FcRn did not disrupt the specificity for trafficking IgG in the transcytotic pathway or for the normal sorting of IgG away from lysosomes.

FcRn-EGFP also recycled IgG from the endosomal compartment back to either apical or basolateral membranes. Here, we incubated FcRn-EGFP cell monolayers with NIP-IgG or the IHH mutant at acidic pH to allow uptake from either cell surface. After 1 h, the cell monolayers were cooled on ice and washed at neutral pH to strip IgG bound at the plasma membrane. The cells were then returned to 37°C and chased for an additional hour in fresh buffer lacking IgG. FcRn-EGFP cells recycled IgG but not IgG-IHH from both cell surfaces, with a greater mass of IgG recycled via the apical membrane (Fig. 1 d). In such pulse-chase studies, we observed progressively increasing transcytosis and recycling of IgG from the basolateral surface, with a corresponding

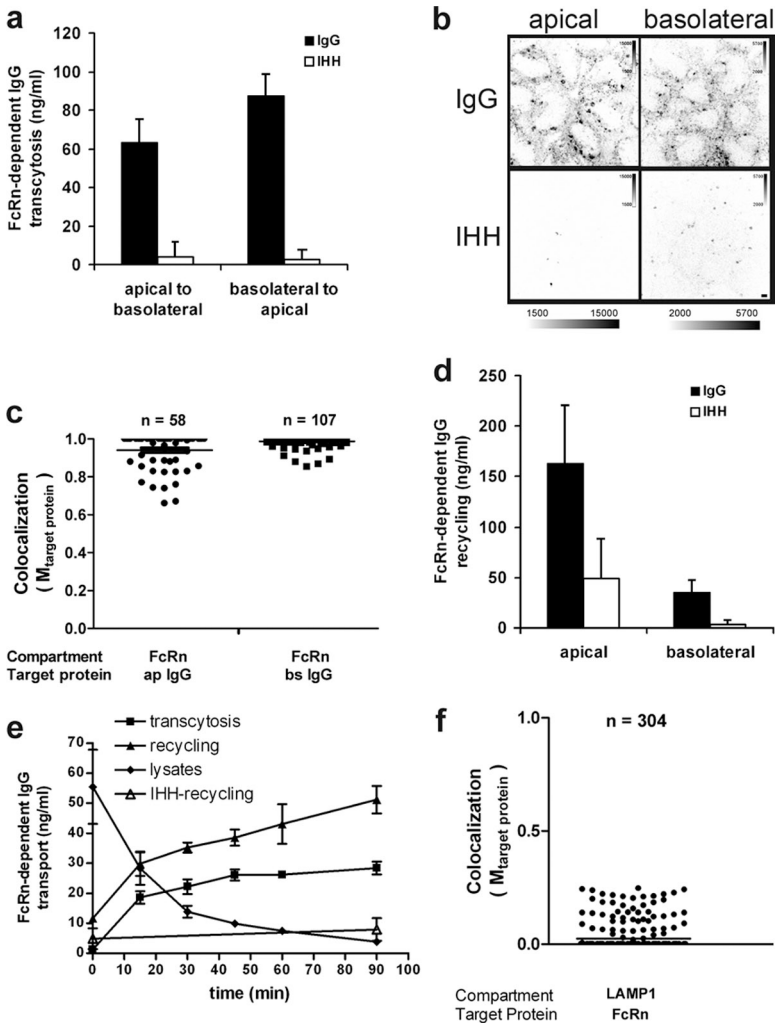

Figure 1. **The fusion protein FcRn-EGFP transports IgG normally in polarized MDCK cells.** (a) FcRn-EGFP–mediated transcytosis of NIP-IgG (shaded bars) or mutant NIP-IgG-IHH (open bars) across MDCK cell monolayers measured by NIP-specific ELISA, as described in Materials and methods. Results shown are mean ± SD (n = 4; ANOVA of IgG vs. IHH, $P < 0.0002$). (b) FcRn-EGFP mediates endocytosis of Alexa Fluor 647–IgG but not Alexa Fluor 647–IgG–IHH from either apical and basolateral surfaces of polarized MDCK cell monolayers, as assessed by confocal microscopy. Intensity scale bars shown demonstrate that images between IgG and IHH were equally contrasted. Bar, 5 μm. (c) IgG is present in FcRn-containing compartments. Cells were incubated with Alexa Fluor 647–IgG as described in panel b and imaged by 3D confocal microscopy. Compartments occupied by both proteins were quantified by first identifying FcRn-EGFP– and IgG-containing objects using an automatic threshold-finding algorithm, and analyzing the colocalization between FcRn-EGFP and IgG using the Manders colocalization coefficient (termed $M_{target\ protein}$, see Materials and methods). The distribution of colocalization $M_{target\ protein}$ for IgG (Target protein) in each FcRn-identified object (Compartment) is shown (data were collected from 40–50 cells of three independent experiments). The horizontal bars indicate a mean $M_{target\ protein}$ of 0.95 and 0.98 for apically applied IgG (ap IgG) and basolaterally applied IgG (bs IgG), respectively. (d) FcRn-EGFP recycles NIP-IgG (shaded bars) or NIP-IgG-IHH (open bars) after endocytosis from either the apical or basolateral surfaces. In brief, as described in Materials and methods, FcRn-EGFP cell monolayers were incubated with NIP-IgG or the IHH mutant at acidic pH to allow uptake from either cell surface for 1 h. IgG bound at the plasma membrane was removed by washing cells at neutral pH at 4°C. The monolayers were then returned to 37°C and chased for an additional hour in fresh buffer lacking IgG. Results shown are mean ± SD (n = 4, ANOVA for IgG vs. IHH, $P < 0.03$). (e) Time course of FcRn-EGFP–mediated NIP-IgG basolateral-to-apical transcytosis, recycling, and cell-associated IgG. Individual monolayers were loaded with NIP-IgG or the IHH mutant for 1 h, and surface IgG was stripped at 4°C. The monolayers were then returned to fresh buffer at 37°C and chased for the indicated times to measure recycling (closed triangles), transcytosis (squares), and total IgG cell-associated content (diamonds). Recycling of NIP-IgG-IHH to the basolateral membrane is also shown as control (open triangles). A representative experiment where each point represents the mean of three separate measurements is shown. Error bars indicate the SD of three independent experiments. (f) FcRn is mostly excluded from the lysosomal compartment. Polarized cells were fixed and immunostained for LAMP1. The distribution of colocalization $M_{target\ protein}$ for FcRn (Target Protein) in each LAMP1-identified object (Compartment) is shown. The horizontal bar indicates mean $M_{target\ protein}$ = 0.02.

decrease in the intracellular content of IgG over time (Fig. 1 e, closed symbols). About 40% of internalized IgG is delivered to the contralateral reservoir, and 50% was recycled after 1 h of loading. Uptake and transport of IgG-IHH was extremely low, showing specificity for FcRn-dependent transport (Fig. 1 e, open triangles). These data validate the MDCK/FcRn-EGFP cell as a model for studies on FcRn function.

FcRn traffics IgG into the common RE

To test whether FcRn is found in the RE of polarized cells, we first examined fixed FcRn-EGFP–expressing cells immunostained for Tf-R by confocal microscopy in 3D, and analyzed them as described for Fig. 1. Nearly all of the Tf-R–defined structures contained FcRn-EGFP throughout the volume of the vesicles analyzed (Fig. 2, a and b, left, mean $M_{target\ protein}$ = 0.97). In contrast, FcRn-defined structures showed a far more varied distribution of overlap with Tf-R (Fig. 2 b, right, mean $M_{target\ protein}$ = 0.64). These results are consistent with the presence of FcRn in apical early endosomes that lack Tf-R, as well as in the basolateral early endosomes and REs that are typified by Tf-R content (Wang et al., 2000a). Nearly identical results were obtained in cells expressing FcRn lacking GFP (unpublished data; and see Claypool et al., 2002).

We next tested if FcRn carries IgG from both cell surfaces into a common RE compartment. For this study, we used FcRn-EGFP cells incubated simultaneously with apically and basolaterally applied IgG (Ap-IgG and Bs-IgG, respectively) labeled with different fluorophores. Fixed cells were imaged by 3D confocal microscopy, and analyzed as described (Fig. 2, c and d). After 60 min of uptake, 78% of FcRn-EGFP–defined structures contained some Ap-IgG (Fig. 2 d, left, mean $M_{target\ protein}$ = 0.58; and Fig. 2 f, left), with a fraction of these objects (37%) colocalizing almost completely with Ap-IgG. A minor fraction (22%) had no detectable Ap-IgG content, which was consistent with lower levels of IgG uptake from the apical cell surface, or with endosomal compartments that contain FcRn but are inaccessible to Ap-IgG. In contrast, almost all FcRn-EGFP–defined structures were occupied by basolaterally applied Bs-IgG (Fig. 2 d, middle, mean $M_{target\ protein}$ = 0.995). When FcRn-EGFP–defined structures

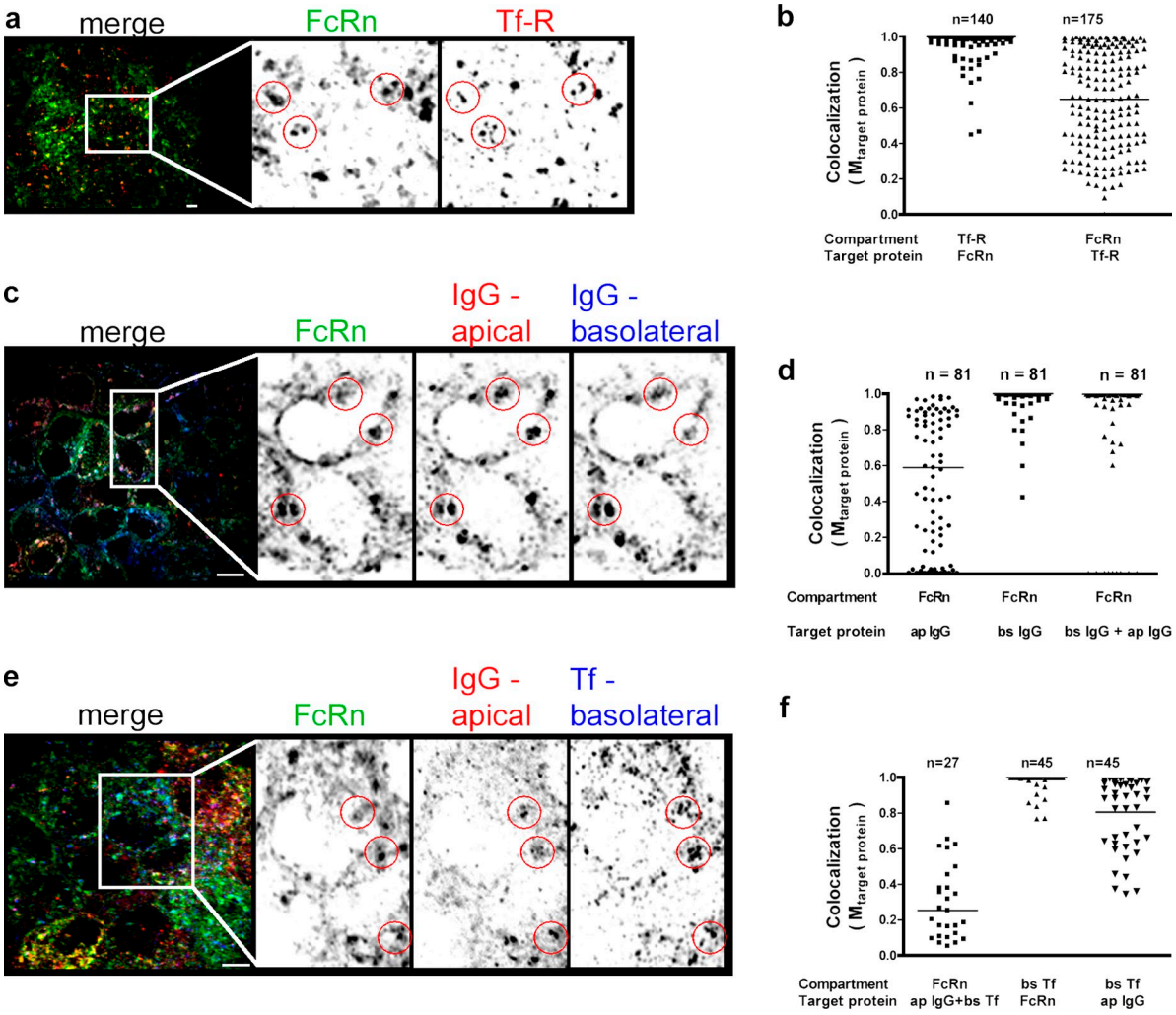

Figure 2. **FcRn transports IgG into the common endosome.** Compartments from 15–40 FcRn-EGFP polarized cells from 3D confocal images were analyzed for content of indicated markers as described in Fig. 1 and the Materials and methods section. Representative images are shown in panels a, c, and e. Panels b, d, and f show quantification of each analysis, with the number of objects studied indicated. Horizontal bars in the graphs indicate mean $M_{target\ protein}$. (a and b) Compartments masked for FcRn-EGFP or Tf-R show a fraction of endosomes containing both molecules. (c and d) Compartments masked for FcRn-EGFP show a fraction containing IgG internalized from both apical and basolateral membranes. Alexa Fluor 568–IgG and Alexa Fluor 647–IgG were applied to apical or basolateral membranes for 1 h, respectively. (e and f) Compartments masked for FcRn-EGFP show a fraction containing IgG internalized from the apical membrane and Tf internalized from the basolateral membrane. Alexa Fluor 568–IgG and Alexa Fluor 647–Tf were applied to apical or basolateral membranes for 1 h, respectively. In a, c, and e, the panels to the right show enlarged views of the boxed portions on the left. Circles highlight the same object in each panel. Bars, 10 µm.

were analyzed for Ap- and Bs-IgG together, thus marking the common RE as operationally defined, two populations were identified. One contained both Ap- and Bs-IgG together, and the minor fraction (11%) did not, presumably representing basolateral early endosomes loaded with Bs-IgG only (Fig. 2 d, right; and inferred from data in Fig. 2 d, left and middle). Nearly the same results were obtained in cells incubated with IgG for only 15 min, which indicates that transport into a common compartment occurs rapidly.

We also measured FcRn trafficking into the RE using Alexa Fluor–labeled Tf to mark the compartment. Here, we allowed FcRn-EGFP cells to internalize IgG from the apical membrane (Ap-IgG) and Tf from the basolateral membrane. After 60 min of uptake, almost all FcRn-EGFP–defined structures contained a fraction of both proteins, but the degree of colocalization was widely varied and often low (Fig. 2, e and f, left, mean $M_{target\ protein} = 0.255$). Some of these structures (22%), however, showed strong overlap (Fig. 2 b, right). When analyzed in reverse, by masking the Tf-defined structures and measuring colocalization with IgG and FcRn-EGFP, we find that almost all Tf-defined structures strongly overlapped with FcRn-EGFP, and all contained Ap-IgG (Fig. 2 f, middle and right, mean $M_{target\ protein} = 0.985$ and 0.805, respectively). Nearly identical results were obtained for cells incubated with both proteins for only 15 min (unpublished data). Thus, FcRn rapidly carries IgG from either apical and basolateral cell surfaces into a common RE.

MyoVb dominant-negative mutant blocks FcRn-dependent IgG transcytosis but not recycling

In addition to the common RE, a specialized endosome termed the ARE has been proposed to regulate trafficking to and from

the apical cell surface only. One of the components thought to regulate the ARE is the motor protein MyoVb. Thus, to test whether the ARE functions to establish the polarity of transport for FcRn in the apically directed pathway, we inhibited MyoVb. To do this, we prepared stable clones of tetracycline repressor (TetR)-FcRn MDCK cells conditionally expressing a dominant-negative mutant MyoVb that lack the motor domain (MyoVb-tail) fused to EGFP. This dominant-negative mutant causes the aggregation of endosomes and disruption of protein trafficking out of the ARE (Lapierre et al., 2001). In the absence of doxycycline, the cells did not express MyoVb tail at detectable levels, as assessed by immunoblotting using antibodies against EGFP or by 3D confocal microscopy (Fig. 3 a, lanes 1 and 2; microscopy data not depicted). Cells treated with doxycycline expressed the MyoVb tail (Fig. 3 a, lanes 3 and 4), which induced the collapse of a Rab11a-containing compartment into a dense apically located structure that excluded the Tf-R; this is consistent with the ARE as operationally defined (Fig. 3 b). When tested functionally, expression of the MyoVb tail inhibited FcRn-dependent IgG transcytosis by ~40% in both directions (Fig. 3 c). Recycling of IgG after apical or basolateral uptake, however, was not affected by expression of the MyoVb tail (Fig. 3 d, shaded bars), and neither was FcRn-mediated endocytosis (Fig. 3 e, shaded bars, compare + and −dox). In all assays, little or no transport of the mutant IgG-IHH was detected under any condition, which confirmed the specificity for FcRn-dependent transcytosis, endocytosis, and recycling (Fig. 3, c–e, open bars). Endocytosis of IgG at shorter time points was below detectable levels, as we have observed previously (Claypool et al., 2004).

Though transcytosis was inhibited, expression of the EGFP–MyoVb tail did not alter the level of FcRn expression as assessed by immunoblotting of total cell lysates (Fig. S2 a), or the level of basolateral polarity of FcRn expression at apical or basolateral membranes at steady-state as assessed by selective cell surface biotinylation (see Materials and methods and Fig. S2 b). Specificity for labeling only apical or basolateral membrane FcRn was demonstrated by analyzing for the apical membrane protein GP135 and the basolateral membrane protein E-cadherin (Fig. S2 c).

Expression of MyoVb tail, however, did cause a fraction of FcRn to condense along with MyoVb into an apically located structure consistent with the ARE (Fig. 4 a), as described in pIgR transport pathways. To test if FcRn also carried IgG into this structure, we allowed FcRn-expressing MDCK cells to internalize Alexa Fluor 568– or Alexa Fluor 647–IgG from apical or basolateral membranes, respectively, and analyzed for colocalization with the MyoVb tail–induced compartment. Starting 15 min after uptake, a progressively greater fraction of apically applied IgG or basolaterally applied IgG was found colocalized with MyoVb tail (Fig. 4 b, compare scatter plots on the left, middle, and right over time). Thus, IgG internalized by FcRn from both cell surfaces populates the MyoVb tail–induced compartment, which is consistent with a regulatory effect of the MyoVb tail on trafficking into or out of this structure (Lapierre et al., 2001). Overexpression of the MyoVb tail, however, had only a small effect, if any, on lysosomal transport as assessed by immunostaining for FcRn and LAMP1 (Fig. S1). Here, the distribution of FcRn-defined objects colocalizing with LAMP1 is uniformly very low (Fig. 3 f, mean $M_{target\ protein}$ = 0.04 and 0.08 for −Dox and +Dox, respectively).

These studies show that MyoVb regulates a sorting step emerging from the RE that is rate-limiting for transcytosis of FcRn in both directions across polarized epithelial cells. These results are not consistent with MyoVb regulating traffic through an endosomal compartment restricted to trafficking with the apical membrane, as operationally defined for the ARE. We also find that inhibition of transcytosis by the MyoVb mutant does not increase recycling of FcRn or transport to the lysosome, which indicates that these trafficking pathways are distinct and do not interact.

FcRn-mediated transcytosis depends on Rab25 and basolateral recycling on Rab11a

Both Rab25 and Rab11a interact with the myosin motor MyoVb, and like MyoVb, they functionally affect trafficking of pIgR through the ARE to the apical membrane (Casanova et al., 1999; Wang et al., 2000a). We separately silenced these genes in FcRn-EGFP cells by conditional expression of small hairpin RNA (shRNA) specific to either Rab11a or Rab25 mRNA. Doxycycline-induced expression of shRNA against these proteins caused almost complete silencing of gene expression, as assessed by RT-PCR for Rab25 (Fig. 5 a) and immunoblotting for Rab11a (Fig. 5 b). Neither cell surface and total expression of FcRn-EGFP nor monolayer polarity and tight junction integrity were affected (Fig. S2, a–c). Gene silencing of Rab25 and Rab11a also had no effect on FcRn-dependent transport of Ap-IgG into REs, as assessed by colocalization with internalized Tf (Fig. 5, c and d) and by colocalization with basolaterally internalized IgG (not depicted).

Gene suppression of Rab25 in FcRn-EGFP cells, however, inhibited IgG transcytosis in both directions by 25–50%, with a greater degree of inhibition in the apical-to-basolateral pathway (Fig. 5 e). Recycling was not detectably affected for IgG entering the cell from either cell surface (Fig. 5 g), and lysosomal transport was not affected, as assessed by colocalization with LAMP1 at steady-state (Fig. 5 i, mean $M_{target\ protein}$ = 0.04 and 0.02 for −Dox and +Dox, respectively; and see Fig. S1 for original micrographs). These results recapitulate our results using MyoVb tail (Fig. 3, c and d) and further suggest that the transcytotic, lysosomal, and recycling pathways are distinct.

In contrast to Rab25, gene suppression of Rab11a had no detectable effect on IgG transcytosis (Fig. 5 f). However, depletion of Rab11a inhibited FcRn-dependent recycling of IgG to the basolateral membrane (Fig. 5 h, compare shaded bars, basolateral −dox and +dox, 40% inhibition). Recycling to the apical membrane was not affected (Fig. 5 h, apical). As with Rab25, lysosomal transport was not affected by silencing Rab11a, as assessed by very low levels of colocalization between FcRn and LAMP1 in cells treated or not treated with doxycycline (Fig. 5 j, mean $M_{target\ protein}$ = 0.03 and 0.02 for −Dox and +Dox, respectively; see Fig. S1 for original micrographs). Thus, Rab11a regulates a sorting step for recycling FcRn to the basolateral membrane, but it is dispensable for transcytosis.

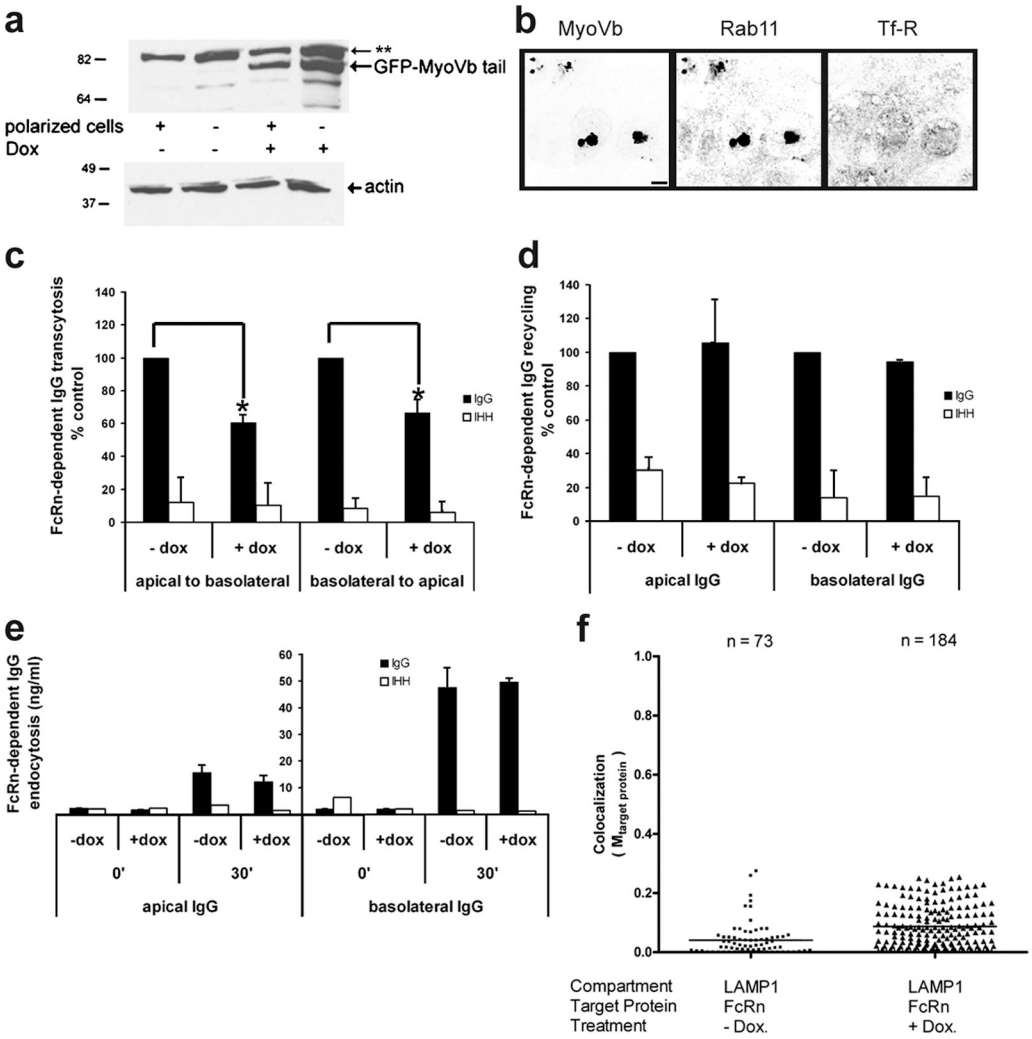

Figure 3. **Overexpression of MyoVb tail blocks FcRn-dependent IgG transcytosis but not recycling.** All experiments were performed in MDCK cells stably expressing a tetracycline-inducible EGFP–MyoVb tail and FcRn-HA. (a) Doxycycline induces expression of EGFP–MyoVb tail in nonpolarized (lanes 1 and 3) and polarized cells (lanes 2 and 4), as measured by SDS-PAGE and immunoblotting using monoclonal antibodies against EGFP. The bottom shows corresponding actin immunoblotting. **, cross-reacting protein band insensitive to doxycycline treatment. Numbers to the left indicate kD. (b) Doxycycline-induced expression of EGFP–MyoVb tail collapses Rab11-containing endosomes into a dense apical structure consistent with the ARE. The induced structure does not contain Tf-R. Polarized cells treated with doxycycline were fixed and immunostained for Rab11 and Tf-R. Bar, 10 µm. (c) Doxycycline-induced expression of EGFP–MyoVb tail inhibits transcytosis of NIP-IgG (shaded bars) in both directions as measured by ELISA; results are mean ± SD (n = 5). NIP-IgG-IHH (open bars) was used as control for nonspecific transport. *, $P < 0.001$. (d) Doxycycline-induced expression of EGFP–MyoVb tail has no detectable effect on recycling of NIP-IgG (shaded bars) to either apical or basolateral cell surfaces as measured by ELISA; results are mean ± SD (n = 3). NIP-IgG-IHH (open bars) is used as a control for nonspecific transport. (e) Doxycycline-induced expression of EGFP–MyoVb tail has no detectable effect on endocytosis of Nip-IgG (shaded bars) from either apical or basolateral membranes. Cells kept on ice (time 0) or incubated with NIP-IgG-IHH (open bars) provide control for nonspecific transport. A representative study with three independent measurements for each point is shown. Error bars indicate the SD of three independent experiments. (f) Doxycycline-induced expression of EGFP–MyoVb tail does not divert FcRn to the lysosomal compartment. Polarized cells treated or not treated with doxycycline were fixed and immunostained for FcRn (HA staining) and LAMP1. The distribution of colocalization of FcRn with LAMP1 was quantified using the Manders coefficient as described (see main text and Materials and methods). Horizontal bars in the graphs indicate that mean $M_{target\ protein}$ equals 0.04 and 0.08 for +Dox and −Dox, respectively.

Because such inhibition of basolateral recycling pathways by Rab11a was not predicted by the results of previous studies on the Tf-R (Wang et al., 2000b), we also examined Tf recycling. Here, to ensure specificity for the Tf-R pathway, we transiently expressed the human isoform of Tf-R in EGFP-FcRn MDCK cell monolayers and conditionally silenced Rab11a or Rab25 as described in the preceding section. Basolateral recycling of ^{125}I-labeled Tf or Alexa Fluor–labeled Tf was assessed by loading the RE with Tf for 90 min at 18°C, washing the cells at low pH at 4°C to dissociate Tf bound to the cell surface, and chasing the monolayers with unlabeled Tf in fresh buffer at 37°C as described previously (Sheff et al., 1999). The time course for recycling to the basolateral membrane was measured by quantitative microscopy (unpublished data) or by gamma counting of samples taken at the indicated times from the basolateral reservoir. Transcytosis of [^{125}I]Tf to the apical membrane was assessed by sampling the apical reservoir, and cell-associated Tf was assessed by gamma counting the entire monolayer at the end of the experiment. The results show by both methods that silencing Rab11a or Rab25 had no detectable effect on the rate of Tf recycling (radioisotope studies are shown in Fig. S3). These results are consistent with previous studies on Tf that used

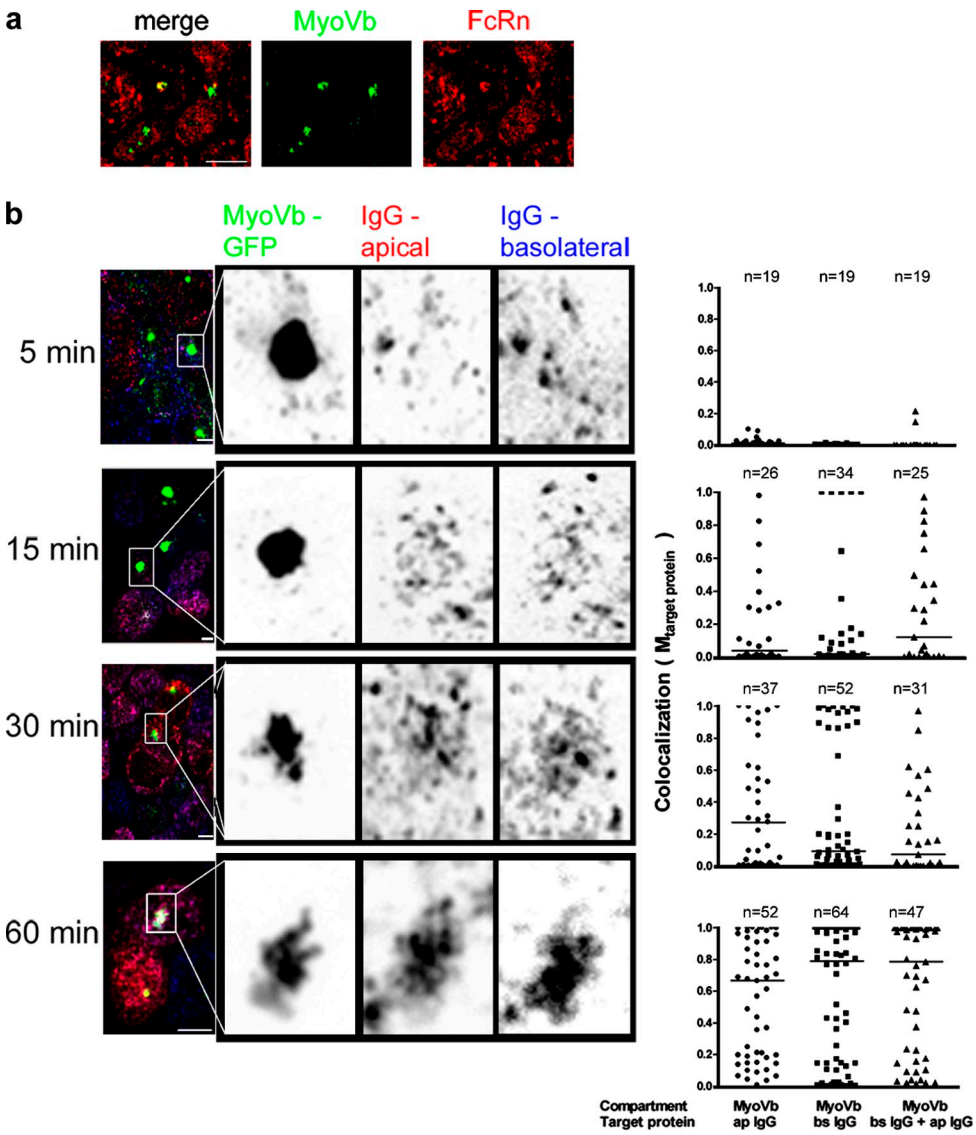

Figure 4. **FcRn transports IgG through the MyoVb tail–induced compartment.** (a) FcRn partially localizes with the EGFP–MyoVb tail, as assessed in fixed cells stained for FcRn-HA. (b) Time course studies show that IgGs entering cells from apical or basolateral surfaces eventually accumulate in the EGFP–MyoVb tail–induced compartment. Alexa Fluor 568–IgG and Alexa Fluor 647–IgG were added at the apical and basolateral reservoirs, respectively; cells were incubated for 5, 15, 30, or 60 min, then fixed and imaged by confocal microscopy. Objects were defined based on the intensity of the EGFP–MyoVb tail; then, the colocalization of apically applied IgG (ap IgG), basolaterally applied IgG (bs IgG), or both IgGs was measured and quantified as described (see Materials and methods). In the micrographs, the panels on the right show enlarged views of the boxed portions on the left. The horizontal bars in the graphs indicate mean $M_{target\ protein}$. Bars, 10 µm.

dominant-negative mutants to inhibit Rab11a function (Wang et al., 2000b), but they contrast with our studies on FcRn. Thus, Rab11a appears to act at a specific juncture in the basolateral recycling pathways that affects FcRn but not Tf-R transport. This result is consistent with the differential recycling of Tf-R and glucose transporter Glut4 from the RE in CHO cells (Lampson et al., 2001), and provides further evidence for the presence of separate recycling pathways originating from the same endosomal compartment.

Discussion

This study shows that the RE in polarized cells sorts FcRn to both cell surfaces via distinct recycling and transcytosis pathways. We conclude this based on our observation that FcRn localizes to the RE, and that MyoVb and Rab25 regulate a sorting step that specifies transcytosis for FcRn in both directions without affecting their recycling. Rab11a, however, perhaps the most well-characterized regulator of the RE, is dispensable for transcytosis of FcRn, and affects receptor-mediated recycling of IgG only in the basolateral pathway. Because blocking the MyoVb and Rab25 sorting steps does not reverse transport back to the membrane of origin, it appears that the epithelial cell can somehow distinguish FcRn moving in opposite directions through common endosomal compartments. The same is true for the basolateral recycling pathway; blocking Rab11a does not force IgG–FcRn complexes into vesicles targeted to the apical membrane. These results provide evidence of a structurally

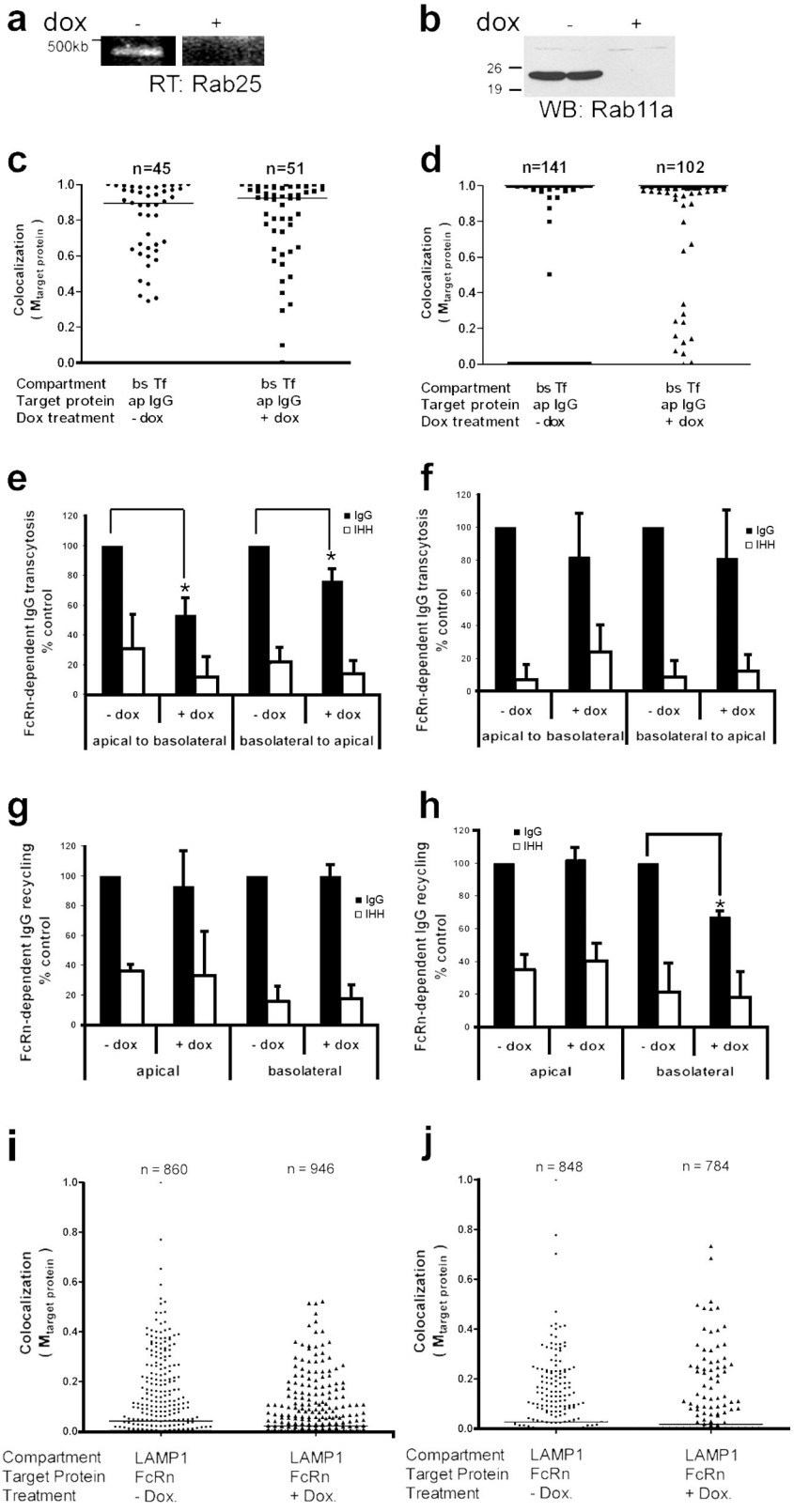

Figure 5. **Rab25 regulates a sorting step that specifies transcytosis, whereas Rab11a regulates recycling in the basolateral pathway only.** All experiments use doxycycline-induced shRNA against Rab25 (left panels) or Rab11a (right panels) in polarized FcRn-EGFP cells. (a) shRNA against Rab25 suppresses gene expression as assessed by RT-PCR. (b) shRNA against Rab11a suppresses gene expression as assessed by SDS-PAGE and immunoblotting. Numbers on the left indicate kD. (c and d) Gene suppression of Rab25 (c) or Rab11a (d) does not alter trafficking of FcRn–IgG complexes into the common RE. Alexa Fluor 568–IgG was applied apically and Alexa Fluor 647–Tf was applied basolaterally for 60 min; they were then fixed and imaged by confocal microscopy. Scatter plots show the degree of colocalization of IgG with Tf. The horizontal bars in the graphs indicate mean $M_{\text{target protein}}$. (e and f) Gene suppression of Rab25 (e) but not Rab11a (f) inhibits transcytosis of NIP-IgG (shaded bars) in both directions across the cell. NIP-IgG-IHH is used as control. Results are mean ± SD. (e, $n = 6$; f, $n = 4$). (g and h) Gene suppression of Rab11a inhibits NIP-IgG (shaded bars) recycling in the basolateral direction only. NIP-IgG-IHH (open bars) is used as control. Results are mean ± SD ($n = 4$). *, $P < 0.001$. (i and j) Doxycycline-induced silencing of Rab25 or Rab11a does not divert FcRn to the lysosomal compartment. Polarized cells treated or not treated with doxycycline were fixed and immunostained with LAMP1. The degree of colocalization of FcRn with LAMP1 was estimated using the Manders coefficient as described (see Materials and methods). Bar indicates mean $M_{\text{target protein}}$.

and functionally heterogeneous RE acting to sort FcRn and other cargoes among distinct recycling and transcytotic pathways in a strongly polarized manner. Evidence for separate transcytotic and recycling pathways originating from the RE was also recently obtained in studies on the chicken yolk sac IgY receptor expressed in MDCK cells (Tesar et al., 2008). In that study, transcytosis of IgY, but not recycling, was dependent on microtubules, which suggests different pathways.

Transit of pIgR through specialized regions of the endosomal compartment during transcytosis has been defined by

dependence on MyoVb, Rab25, and Rab11a (Casanova et al., 1999; Wang et al., 2000a; Lapierre and Goldenring, 2005). All three components act downstream of endocytosis and transport into the basolateral early endosome and common RE, and they are also required for trafficking of pIgR to the apical membrane. Except for the lack of dependence on Rab11a function, our results are consistent with the studies on pIgR. We find, however, that MyoVb and Rab25 regulate transcytosis in both directions across the cell. This is an observation that could never be made in studies on pIgR, which travels physiologically in only one direction across epithelial barriers; and it is the first line of evidence that Rab25 and MyoVb participate in transport of cargo to basolateral membranes. This result does not support the concept of an exclusive endosomal compartment dedicated to apical membrane trafficking (the ARE as currently defined), and it is more consistent with the two-compartment model for endosomal sorting in polarized cells (Sheff et al., 1999). Our experimental system is particularly robust in this respect, as we measure trafficking in both directions using the same protein, FcRn. The results of these studies, however, do support the accumulating evidence that the RE contributes significantly to structure and function of the apical membrane in polarized epithelial cells (Forte et al., 1990; Tajika et al., 2004; Wakabayashi et al., 2005; Swiatecka-Urban et al., 2007; Muller et al., 2008). MyoVb and Rab25 also affect transport of FcRn to the opposite basolateral membrane, which is consistent with the concept of a structurally and functionally heterogeneous RE regulating membrane transport to both cell surfaces.

Why the transcytosis of FcRn to the apical membrane differs from pIgR and does not require Rab11a might be explained by recent studies on the domain structure of the Rab11a- and MyoVb–interacting protein Rab11-FIP2. Different mutations in Rab11-FIP2 affected the transcytotic pathway for IgA in different ways, which suggests multiple sorting steps for transcytosis in the basolateral-to-apical direction for pIgR (Ducharme et al., 2007). It is possible that FcRn takes one pathway and pIgR another.

We also find that in contrast to pIgR, FcRn does not recycle via endocytic compartments regulated by MyoVb and Rab25. For recycling to the basolateral membrane, FcRn uses a pathway dependent on Rab11a, apparently originating from the RE and distinct from Tf-R (this paper and Wang et al., 2000a). This is consistent with evidence that the RE can differentially sort membrane proteins in the recycling pathway (Lampson et al., 2001). Furthermore, such transport to the basolateral membrane via a Rab11a-dependent sorting step in the RE has been described for E-cadherin (Lock and Stow, 2005; Desclozeaux et al., 2008), and it is possible that FcRn uses the same system. MyoVb tail has no effect on E-cadherin trafficking, which is consistent with such a pathway (Ducharme et al., 2006). FcRn does not require Rab11a for recycling at the apical cell surface, which suggests that this event originates from a different compartment, possibly the apical early endosome, and is perhaps regulated by Rab4 (Ward et al., 2005) or the exocyst complex (Oztan et al., 2007). Another possibility is that a small fraction of apical recycling for FcRn also originates from the RE via rab17 (Zacchi et al., 1998) or Rab11a-FIP5/Rip11–regulated pathways (Prekeris et al., 2000; Schonteich et al., 2008), but this is below detection by our methods.

None of the regulatory molecules studied here had effects on sorting steps that protect FcRn from transport into the lysosome. This is understandable if sorting into the lysosomal pathway for FcRn originates from the early endosome upstream of the RE, as for other membrane and soluble proteins (Maxfield and McGraw, 2004). Under all conditions, we found only a very small fraction of FcRn localized to lysosomal compartments at steady-state, considerably less than that observed for the rat isoform of FcRn expressed in MDCK cells (Tesar et al., 2006). Why the human isoform appears to sort more efficiently away from lysosomes remains unexplained for now, but this typifies FcRn function in vivo. The distal cytoplasmic tail domains of human and rat FcRn do not show sequence homology, and perhaps this affects sorting in the lysosomal pathway. A recent paper shows that IgG binding to FcRn diverts a fraction of the IgG–FcRn complex into the lysosome of human endothelial cell line HMEC-1 (Gan et al., 2009). The experiments described in our studies do not address this question, but like Tesar et al., (2006), we did not find such an effect on IgG binding to human FcRn in MDCK cells (unpublished data).

Overall, the location of FcRn in a common endosome shared with apically and basolaterally internalized cargoes and Tf, and the dependence on MyoVb and Rab25 for FcRn transport, identify the RE as a critical sorting station for both transcytotic pathways in polarized epithelial cells. Perhaps these rate-limiting steps for transcytosis explain why the bulk of FcRn localizes to this compartment at steady-state in epithelial as well as in endothelial cells (Ward et al., 2005)). But what, then, are the polarity determinants explaining how FcRn is moved in the correct direction, apical or basolateral, within a common RE? One possibility suggested previously (Sheff et al., 1999; Hoekstra et al., 2004; Maxfield and McGraw, 2004; Thompson et al., 2007) is that the RE represents a structurally and functionally heterogeneous compartment, with membrane domains dedicated to receiving and distributing membrane components to one cell surface or the other. In fact, the very first studies describing the RE in polarized cells provide evidence for basolateral polarity in the direction of Tf-R transport through this compartment (Odorizzi et al., 1996), consistent with our results on trafficking FcRn. The structural complexity of the recycling endosomal compartment, which is capable of trafficking FcRn among different pathways, is perhaps most clearly visualized in recent ultrastructural studies on epithelial cells lining the proximal intestine of the neonatal mouse, which are specialized for IgG transport by FcRn (He et al., 2008). Here, FcRn is found localized to endosomes of diverse morphology and presumably diverse functions.

Some structural information driving polarity in a bidirectional pathway must also be encoded with FcRn itself or by associated molecules. Apical and basolateral plasma membranes exhibit vast differences in their lipid and protein composition, and this might cause FcRn at the cell surfaces to assemble with different membrane components that affect the direction of transport. Another plausible explanation is that the polarity of transport might be encoded by reversible structural changes in FcRn. Serine/threonine-based motifs present in the FcRn cytoplasmic tail, for example, suggest cycles of phosphorylation and dephosphorylation. Consistent with this idea, McCarthy et al., (2001) have shown in rat kidney cells that mutation of the FcRn cytoplasmic

tail at serine 313 inhibits transcytosis of IgG in the apical-to-basolateral direction only. Cross-linking FcRn by IgG can also account for sorting itineraries within the endosomal compartment (Kim et al., 1994; Raghavan and Bjorkman, 1996; Tesar et al., 2006; Qiao et al., 2008), and perhaps this can operate to establish the direction of transport as well. Several mechanisms, of course, might operate in parallel or in sequence. Based on our results, we propose that such sorting events occur via structurally different subdomains in the RE, and that these are the decisive factors explaining how recycling and bidirectional transcytosis of FcRn can be differentially regulated in polarized cells.

Materials and methods

Plasmids

Monomeric EGFP was fused to the FcRn C terminus with a GSSGSS linker between FcRn and EGFP (pcDNA3.1; Invitrogen). The FcRn-EGFP fusion was transfected into MDCKII cells stably expressing human β_2M (Claypool et al., 2002). Clones were selected using 0.5 mg/ml G418 (Meditech, Inc.). The TetR was cloned from pcDNA6/TR (Invitrogen) into the retroviral vector pQCXiH (Invitrogen) using BsiWI and PacI. pQCXiH-TetR was transfected into Phoenix HEK293 cells using FuGene6 (Roche). Cells were fed after 24 h; medium containing retroviruses was collected 48 h later, then filtered and transfected to either EGFP-FcRn or wild-type FcRn cells. The cells were selected using 200 µg/ml hygromycin (Meditech, Inc.). MyoVb tail was cloned as described previously (Lapierre et al., 2001). The EGFP–MyoVb tail was inserted into pcDNA4/TO (Invitrogen) under cytomegalovirus promoter containing two tetracycline operon2 sites using NotI and XbaI, and transfected into TetR-FcRn cells using Lipofectamine 2000 (Invitrogen). The cells were selected using 400 µg/ml zeocin (Invitrogen).

Vector-based shRNA gene suppression cloning

The system for conditional shRNA-based knockdown of gene expression in MDCK cells, including the tetracycline-inducible pReSI-H1 vector and the shRNA design protocol, was developed by S.H. Hansen and S.R. Frank. In brief, complimentary 80-bp oligonucleotides containing BamH1 and HindIII overhangs were annealed and inserted into pReSI-H1. Rab11a shRNA: 5′-GCAGTGCTGTCAGAACATATA-3′; Rab25 shRNA: 5′-CTCAAAGGCTAGCTCAACATT-3′. pResI-Rab11a-shRNA or pResI-Rab25-shRNA were then transfected into Phoenix HEK293 cells using FuGene6, and virus-containing medium was used to infect TetR-EGFP-FcRn cells as described previously. The cells were selected using 2.5 mg/ml puromycin (EMD).

Cell culture

Cell culture media was obtained from Invitrogen. Culture dishes and Transwell filter plates were obtained from Corning. To express MyoVb, cells were cultured in a plate for 2 d in the presence of 4 µg/ml doxycycline (Sigma-Aldrich) and then replated into Transwell filters for an additional 3 d in the presence of doxycycline; or, in some experiments, the cells were plated on Transwell filters and treated with doxycycline 24 h after plating. Both methods gave identical results. To induce gene suppression of Rab11a or Rab25, cells were plated into Transwell filters for 4 d in the presence of 4 µg/ml doxycycline. Although it has been shown by dominant-negative inhibition that Rab11a is required for E-cadherin sorting and establishment of polarity (Lock and Stow, 2005; Desclozeaux et al., 2008), the methods we used here by gene silencing after plating cells at near confluency allow for the formation and maintenance of polarized tight monolayers, as indicated by transepithelial resistance, IgG transport, and selective cell surface biotinylation of apical and basolateral membrane proteins (Fig. S2).

Antibodies (Ab)

Human IgG was obtained from Lampire Biological Laboratories, and was labeled with Alexa Fluor 568 or 647 using molecular probe kits (Invitrogen) according to the manufacturer's instructions. HRP-conjugated goat anti–human IgG was obtained from Jackson ImmunoResearch Laboratories. Monoclonal Ab 12CA5, which is reactive against the HA epitope, has been described previously (Claypool et al., 2002). High-affinity rat anti-HA mAb was obtained from Roche. Mouse mAbs against β-actin and HRP-conjugated secondary antibodies were obtained from Sigma-Aldrich. Rab11 antibodies (mono- and polyclonal) have been described previously (Goldenring et al., 1996). Tf-R mAbs and Rab11 polyclonal Ab were obtained from Invitrogen. LAMP1 mAb was a gift of E. Rodriguez-Boulan (Cornell University, New York, NY). Alexa Fluor–conjugated secondary antibodies were obtained from Invitrogen.

RT-PCR

Polarized cells were grown on Transwell filters, untreated or treated for 4 d with 4 µg/ml doxycycline. The cells were lysed, and total RNA was purified using an SV total RNA isolation kit (Promega). First-strand DNA was synthesized using SuperScript Reverse transcription (Invitrogen) according to the manufacturer's instructions. Canine Rab25 PCR was performed using the forward primer 5′-AAGGCTCAGATCTGGGACACA-3′ and the reverse primer 5′-GTGCTGTTCTGCCTCTGCTT-3′, and gave a product of 400 kb.

NiP-IgG purification

Recombinant human NIP-specific IgG and NIP-IgG-IHH were produced by J558L myeloma cells and purified from the cell media using affinity chromatography on a NIP-sepharose column (Biosearch Technologies), then eluted with 100 mM ethanolamine and neutralized with 100 mM Tris base, pH 6.8. The eluate was concentrated using Centriprep (Millipore) and dialyzed against PBS.

Transcytosis, recycling, and endocytosis

Transcytosis of NIP-IgG or NIP-IgG-IHH across monolayers was performed in triplicate using three independent monolayers as described previously (Claypool et al., 2004). In brief, cells were washed with HBSS containing 10 mM Hepes, pH 7.4, serum starved for 20 min, and then washed with HBSS containing 23 mM MES, pH 6.0, for 10 min. 10 µg/ml NIP-IgG or NIP-IgG-IHH was added at either the apical or basolateral chamber at pH 6.0. For transcytosis, the medium in the contralateral chamber was collected after 120 min of continuous uptake at 37°C. In the recycling experiments described in the following paragraph, transcytosis was measured after 60 min of loading.

For recycling, the cells were loaded with IgG from either apical or basolateral cell surfaces. The cells were then washed thoroughly with ice-cold HBSS, pH 7.4, before returning them to fresh HBSS, pH 7.4, at 37°C for an additional 60 min. The media from both reservoirs (apical and basolateral) was collected to measure recycling.

For endocytosis, the cells were incubated with 50 µg/ml antibodies on ice or at 37°C for 30 min. The cells were lysed with RIPA buffer (50 mM Tris base, pH 8.0, 150 mM NaCl, 0.1% SDS, 1% NP-40, and 0.25% sodium deoxycholate). Antibodies in the transcytosis, recycling, and the post-nuclear lysate fractions were measured using a NIP-specific ELISA, and the means ± SD were plotted.

Selective cell surface biotinylation

Selective cell surface biotinylation was performed as described previously (Casanova et al., 1991). In brief, cells were washed with ice-cold PBS containing Mg^{2+} and Ca^{2+} (PBS+). The apical or basolateral cell surface was then derivatized (twice for 30 min) using 0.5 mg/ml of the nonmembrane-permeating sulfo–*N*-hydroxysuccinimide–biotin (Thermo Fisher Scientific) twice for 30 min at 4°C, and quenched by PBS+ containing 50 mM NH_4Cl. RIPA lysates were incubated with avidin-agarose beads. Biotinylated FcRn was detected by anti-HA immunoblotting.

Immunofluorescence, microscopy, and image analysis

Cells, grown for 4 d on Transwell filters, were fixed with 4% paraformaldehyde (Electron Microscopy Sciences) in PBS for 20 min at 4°C. All remaining steps were performed at room temperature in a humidified chamber. Fixed cells were extensively washed in PBS and permeabilized with 0.2% saponin for 30 min. Nonspecific binding was blocked by incubation with 10% nonimmune goat serum for 30 min (VWR International, LLC). All antibody incubations were performed in the presence of 10% nonimmune goat serum and 0.2% saponin. Alexa Fluor–conjugated, species-specific goat secondary antibodies were diluted at 1:200. The membranes were cut and then mounted using the Prolong Antifade reagent (Invitrogen). 3D images were taken using a spinning disk confocal head (PerkinElmer) coupled to a fully motorized inverted microscope: either an Axiovert 200M (Carl Zeiss, Inc.) or an eclipse TE2000-E (Nikon) equipped with a 100× objective lens (Pan-Apochromat, 1.4 NA; Nikon). A 50-mW solid-state laser (473 and 660 nm [CrystaLaser]; 568 nm [Cobolt]) coupled to the spinning head through an acoustic-optical tunable filter was used as a light source. The imaging system was operated under the control of SlideBook 4.2 (Intelligent Imaging Innovations Inc.) and included a computer-controlled spherical aberration correction device (Motorized InFocus Device; Infinity

Photo-Optical Company and Intelligent Imaging Innovations) installed between the microscope and the confocal head. Images were detected using a back-illuminated charge-coupled device (Cascade 512B; Roper Scientific) or Orca ER (Hammamatsu) camera.

Quantitation of the fraction of a given target protein in a 3D-masked endosomal compartment was determined by the following protocol: (1) Object masks were created by segmenting the compartment's marker protein fluorescent intensity above the local background using an automatic and unbiased threshold finder (Volocity; PerkinElmer; Costes et al., 2004). (2) The colocalization coefficients (Manders et al., 1992) were measured within the masked region using Volocity. These coefficients vary from 0 to 1, the former corresponding to nonoverlapping images and the latter reflecting 100% colocalization between both images. (3) The fraction of a protein contained within a defined compartment (termed $M_{target\ protein}$) was defined as the ratio of the summed of pixels intensities ($M_{target\ protein}$) from the green image (e.g., target protein), for which the intensity in the red channel (compartment protein) is within the selected intensity thresholds, over the sum of all pixel intensities from the green image channel above background. Thus, $M_{target\ protein}$ is a good indicator of the proportion of the green signal coincident with a signal in the red channel over its total intensity. In some experiments, live cells expressing EGFP-FcRn were incubated with 66 nM Lysotracker (Invitrogen) to label lysosomes, and colocalization with EGFP-FcRn was analyzed by confocal microscopy in 3D, as described in the previous two paragraphs.

Tf recycling

MDCK cells stably expressing doxycycline-induced expression of shRNA specific to either Rab11a or Rab25 mRNA were transiently transfected with human Tf-R to ensure the specific uptake of human Tf. The next day, transfected cells were plated onto 24-mm Transwell inserts (0.4 mm pore) at confluence, and incubated for 3 d to polarize. Cells were then incubated at 37°C with warmed serum-free media (HBSS, pH 7.4) for 30 min to deplete already internalized Tf from serum, followed by further incubation with 10 µg/ml ^{125}I-Tf in HBSS supplemented with 1% BSA added for 90 min at 18°C. Surface-bound ^{125}I-Tf was removed by a brief acid wash (pH 6.0, 5 min) at 4°C followed by neutral wash with HBSS, pH 7.4, also at 4°C. A pair of samples for each condition (− or +doxycycline) was immediately lysed to control for internalized ^{125}I-Tf. All other samples were incubated with chasing medium consisting of HBSS (pH 7.4) supplemented with 1% BSA, 100 µM desferrioxamine (Sigma-Aldrich), and 100 µg/ml of unlabeled Tf applied to both chambers. Filters were transferred to new wells containing chasing medium every 5 min for a total of 1 h, and 2 ml of basolateral medium was collected for gamma counting. Upper chamber medium was also collected at the end of the chase to measure total transcytosis. Filters were lysed to measure residual internalized ^{125}I-Tf.

Statistical analysis

Analysis was done with single-factor analysis of variance (ANOVA) to test for significance of IgG and IHH or doxycycline treatment (gene expression or suppression), and to control for the observed interexperiment variation in levels of IgG transport common to all treatment groups, which is due, presumably, to variations in cell culture and passage number.

Online supplemental material

Fig. S1 shows that FcRn sorts away from the lysosome and that neither inhibition of MyoVb nor gene suppression of Rab 25 and Rab11a alters this trafficking. Fig. S2 shows that the expression of a MyoVb mutant or gene suppression of Rab11a or Rab25 has no detectable effect on total and cell surface levels of FcRn. Fig. S3 shows that gene suppression of Rab11a or Rab25 has no detectable effect on basolateral recycling of Tf-R. Online supplemental material is available at http://www.jcb.org/cgi/content/full/jcb.200809122/DC1.

We thank Marianne Wesling-Resnick and Peter Bucket for assistance with the Tf recycling studies, and Yariv Tzaban for technical support with writing original software.

This work was supported by research grants from the National Institutes of Health (RO1 DK53056 to W.I. Lencer and R.S. Blumberg, RO1 DK48370 and DK070856 to J.R. Goldenring, and CA092354 to S.H. Hansen), a Senior Research Grant from the Crohns Colitis Foundation (1842 to W.I. Lencer), and a grant from the Harvard Digestive Diseases Center National Institutes of Health (P30 DK034854).

Submitted: 18 September 2008
Accepted: 15 April 2009

References

Apodaca, G., L.A. Katz, and K.E. Mostov. 1994. Receptor-mediated transcytosis of IgA in MDCK cells is via apical recycling endosomes. *J. Cell Biol.* 125:67–86.

Bitonti, A.J., J.A. Dumont, S.C. Low, R.T. Peters, K.E. Kropp, V.J. Palombella, J.M. Stattel, Y. Lu, C.A. Tan, J.J. Song, et al. 2004. Pulmonary delivery of an erythropoietin Fc fusion protein in non-human primates through an immunoglobulin transport pathway. *Proc. Natl. Acad. Sci. USA.* 101:9763–9768.

Burmeister, W.P., A.H. Huber, and P.J. Bjorkman. 1994. Crystal structure of the complex of rat neonatal Fc receptor with Fc. *Nature.* 372:379–383.

Casanova, J.E., Y. Mishumi, Y. Ikehara, A.L. Hubbard, and K.E. Mostov. 1991. Direct apical sorting of rat liver dipeptidylpeptidase IV expressed in Madin-Darby canine kidney cells. *J. Biol. Chem.* 266:24428–24432.

Casanova, J.E., X. Wang, R. Kumar, S.G. Bhartur, J. Navarre, J.E. Woodrum, Y. Altschuler, G.S. Ray, and J.R. Goldenring. 1999. Association of Rab25 and Rab11a with the apical recycling system of polarized Madin-Darby canine kidney cells. *Mol. Biol. Cell.* 10:47–61.

Claypool, S.M., B.L. Dickinson, M. Yoshida, W.I. Lencer, and R.S. Blumberg. 2002. Functional reconstitution of human FcRn in Madin-Darby canine kidney cells requires co-expressed human β 2-microglobulin. *J. Biol. Chem.* 277:28038–28050.

Claypool, S.M., B.L. Dickinson, J.S. Wagner, F.E. Johansen, N. Venu, J.A. Borawski, W.I. Lencer, and R.S. Blumberg. 2004. Bidirectional transepithelial IgG transport by a strongly polarized basolateral membrane Fcγ-receptor. *Mol. Biol. Cell.* 15:1746–1759.

Costes, S.V., D. Daelemans, E.H. Cho, Z. Dobbin, G. Pavlakis, and S. Lockett. 2004. Automatic and quantitative measurement of protein-protein colocalization in live cells. *Biophys. J.* 86:3993–4003.

Desclozeaux, M., J. Venturato, F.G. Wylie, J.G. Kay, S.R. Joseph, H.T. Le, and J.L. Stow. 2008. Active Rab11 and functional recycling endosome are required for E-cadherin trafficking and lumen formation during epithelial morphogenesis. *Am. J. Physiol. Cell Physiol.* 295:C545–C556.

Dickinson, B.L., K. Badizadegan, Z. Wu, J.C. Ahouse, X. Zhu, N.E. Simister, R.S. Blumberg, and W.I. Lencer. 1999. Bidirectional FcRn-dependent IgG transport in a polarized human intestinal cell line. *J. Clin. Invest.* 104:903–911.

Dickinson, B.L., S.M. Claypool, J.A. D'Angelo, M.L. Aiken, N. Venu, E.H. Yen, J.S. Wagner, J.A. Borawski, A.T. Pierce, R. Hershberg, et al. 2008. Ca2+-dependent calmodulin binding to FcRn affects immunoglobulin G transport in the transcytotic pathway. *Mol. Biol. Cell.* 19:414–423.

Ducharme, N.A., C.M. Hales, L.A. Lapierre, A.J. Ham, A. Oztan, G. Apodaca, and J.R. Goldenring. 2006. MARK2/EMK1/Par-1Bα phosphorylation of Rab11-family interacting protein 2 is necessary for the timely establishment of polarity in Madin-Darby canine kidney cells. *Mol. Biol. Cell.* 17:3625–3637.

Ducharme, N.A., J.A. Williams, A. Oztan, G. Apodaca, L.A. Lapierre, and J.R. Goldenring. 2007. Rab11-FIP2 regulates differentiable steps in transcytosis. *Am. J. Physiol. Cell Physiol.* 293:C1059–C1072.

Dumont, J.A., A.J. Bitonti, D. Clark, S. Evans, M. Pickford, and S.P. Newman. 2005. Delivery of an erythropoietin-Fc fusion protein by inhalation in humans through an immunoglobulin transport pathway. *J. Aerosol Med.* 18:294–303.

Forte, J.G., D.K. Hanzel, C. Okamoto, D. Chow, and T. Urushidani. 1990. Membrane and protein recycling associated with gastric HCl secretion. *J. Intern. Med. Suppl.* 732:17–26.

Gan, Z., S. Ram, C. Vaccaro, R.J. Ober, and E.S. Ward. 2009. Analyses of the recycling receptor, FcRn, in live cells reveal novel pathways for lysosomal delivery. *Traffic.* In press.

Ghetie, V., J.G. Hubbard, J.K. Kim, M.F. Tsen, Y. Lee, and E.S. Ward. 1996. Abnormally short serum half-lives of IgG in β 2-microglobulin-deficient mice. *Eur. J. Immunol.* 26:690–696.

Goebl, N.A., C.M. Babbey, A. Datta-Mannan, D.R. Witcher, V.J. Wroblewski, and K.W. Dunn. 2008. Neonatal Fc receptor mediates internalization of Fc in transfected human endothelial cells. *Mol. Biol. Cell.* 19:5490–5505.

Goldenring, J.R., J. Smith, H.D. Vaughan, P. Cameron, W. Hawkins, and J. Navarre. 1996. Rab11 is an apically located small GTP-binding protein in epithelial tissues. *Am. J. Physiol.* 270:G515–G525.

He, W., M.S. Ladinsky, K.E. Huey-Tubman, G.J. Jensen, J.R. McIntosh, and P.J. Bjorkman. 2008. FcRn-mediated antibody transport across epithelial cells revealed by electron tomography. *Nature.* 455:542–547.

Hoekstra, D., D. Tyteca, and S.C. van Ijzendoorn. 2004. The subapical compartment: a traffic center in membrane polarity development. *J. Cell Sci.* 117:2183–2192.

Israel, E.J., D.F. Wilsker, K.C. Hayes, D. Schoenfeld, and N.E. Simister. 1996. Increased clearance of IgG in mice that lack β 2-microglobulin: possible protective role of FcRn. *Immunology.* 89:573–578.

Junghans, R.P., and C.L. Anderson. 1996. The protection receptor for IgG catabolism is the β2-microglobulin-containing neonatal intestinal transport receptor. *Proc. Natl. Acad. Sci. USA.* 93:5512–5516.

Kim, J.K., M.F. Tsen, V. Ghetie, and E.S. Ward. 1994. Catabolism of the murine IgG1 molecule: evidence that both CH2-CH3 domain interfaces are required for persistence of IgG1 in the circulation of mice. *Scand. J. Immunol.* 40:457–465.

Lampson, M.A., J. Schmoranzer, A. Zeigerer, S.M. Simon, and T.E. McGraw. 2001. Insulin-regulated release from the endosomal recycling compartment is regulated by budding of specialized vesicles. *Mol. Biol. Cell.* 12:3489–3501.

Lapierre, L.A., and J.R. Goldenring. 2005. Interactions of myosin vb with rab11 family members and cargoes traversing the plasma membrane recycling system. *Methods Enzymol.* 403:715–723.

Lapierre, L.A., R. Kumar, C.M. Hales, J. Navarre, S.G. Bhartur, J.O. Burnette, D.W. Provance Jr., J.A. Mercer, M. Bahler, and J.R. Goldenring. 2001. Myosin vb is associated with plasma membrane recycling systems. *Mol. Biol. Cell.* 12:1843–1857.

Lock, J.G., and J.L. Stow. 2005. Rab11 in recycling endosomes regulates the sorting and basolateral transport of E-cadherin. *Mol. Biol. Cell.* 16:1744–1755.

Manders, E.M., J. Stap, G.J. Brakenhoff, R. van Driel, and J.A. Aten. 1992. Dynamics of three-dimensional replication patterns during the S-phase, analysed by double labelling of DNA and confocal microscopy. *J. Cell Sci.* 103:857–862.

Maxfield, F.R., and T.E. McGraw. 2004. Endocytic recycling. *Nat. Rev. Mol. Cell Biol.* 5:121–132.

McCarthy, K.M., M. Lam, L. Subramanian, R. Shakya, Z. Wu, E.E. Newton, and N.E. Simister. 2001. Effects of mutations in potential phosphorylation sites on transcytosis of FcRn. *J. Cell Sci.* 114:1591–1598.

Medesan, C., P. Cianga, M. Mummert, D. Stanescu, V. Ghetie, and E.S. Ward. 1998. Comparative studies of rat IgG to further delineate the Fc:FcRn interaction site. *Eur. J. Immunol.* 28:2092–2100.

Mezo, A.R., K.A. McDonnell, C.A. Hehir, S.C. Low, V.J. Palombella, J.M. Stattel, G.D. Kamphaus, C. Fraley, Y. Zhang, J.A. Dumont, and A.J. Bitonti. 2008. Reduction of IgG in nonhuman primates by a peptide antagonist of the neonatal Fc receptor FcRn. *Proc. Natl. Acad. Sci. USA.* 105:2337–2342.

Muller, T., M.W. Hess, N. Schiefermeier, K. Pfaller, H.L. Ebner, P. Heinz-Erian, H. Ponstingl, J. Partsch, B. Rollinghoff, H. Kohler, et al. 2008. MYO5B mutations cause microvillus inclusion disease and disrupt epithelial cell polarity. *Nat. Genet.* 40:1163–1165.

Odorizzi, G., A. Pearse, D. Domingo, I.S. Trowbridge, and C.R. Hopkins. 1996. Apical and basolateral endosomes of MDCK cells are interconnected and contain a polarized sorting mechanism. *J. Cell Biol.* 135:139–152.

Oztan, A., M. Silvis, O.A. Weisz, N.A. Bradbury, S.C. Hsu, J.R. Goldenring, C. Yeaman, and G. Apodaca. 2007. Exocyst requirement for endocytic traffic directed toward the apical and basolateral poles of polarized MDCK cells. *Mol. Biol. Cell.* 18:3978–3992.

Prekeris, R., J. Klumperman, and R.H. Scheller. 2000. A Rab11/Rip11 protein complex regulates apical membrane trafficking via recycling endosomes. *Mol. Cell.* 6:1437–1448.

Qiao, S.W., K. Kobayashi, F.E. Johansen, L.M. Sollid, J.T. Andersen, E. Milford, D.C. Roopenian, W.I. Lencer, and R.S. Blumberg. 2008. Dependence of antibody-mediated presentation of antigen on FcRn. *Proc. Natl. Acad. Sci. USA.* 105:9337–9342.

Raghavan, M., and P.J. Bjorkman. 1996. Fc receptors and their interactions with immunoglobulins. *Annu. Rev. Cell Dev. Biol.* 12:181–220.

Raghavan, M., L.N. Gastinel, and P.J. Bjorkman. 1993. The class I major histocompatibility complex related Fc receptor shows pH-dependent stability differences correlating with immunoglobulin binding and release. *Biochemistry.* 32:8654–8660.

Rodewald, R. 1976. pH-dependent binding of immunoglobulins to intestinal cells of the neonatal rat. *J. Cell Biol.* 71:666–670.

Rojas, R., and G. Apodaca. 2002. Immunoglobulin transport across polarized epithelial cells. *Nat. Rev. Mol. Cell Biol.* 3:944–955.

Schonteich, E., G.M. Wilson, J. Burden, C.R. Hopkins, K. Anderson, J.R. Goldenring, and R. Prekeris. 2008. The Rip11/Rab11-FIP5 and kinesin II complex regulates endocytic protein recycling. *J. Cell Sci.* 121:3824–3833.

Sheff, D.R., E.A. Daro, M. Hull, and I. Mellman. 1999. The receptor recycling pathway contains two distinct populations of early endosomes with different sorting functions. *J. Cell Biol.* 145:123–139.

Spiekermann, G.M., P.W. Finn, E.S. Ward, J. Dumont, B.L. Dickinson, R.S. Blumberg, and W.I. Lencer. 2002. Receptor-mediated immunoglobulin G transport across mucosal barriers in adult life: functional expression of FcRn in the mammalian lung. *J. Exp. Med.* 196:303–310.

Swiatecka-Urban, A., L. Talebian, E. Kanno, S. Moreau-Marquis, B. Coutermarsh, K. Hansen, K.H. Karlson, R. Barnaby, R.E. Cheney, G.M. Langford, et al. 2007. Myosin Vb is required for trafficking of the cystic fibrosis transmembrane conductance regulator in Rab11a-specific apical recycling endosomes in polarized human airway epithelial cells. *J. Biol. Chem.* 282:23725–23736.

Tajika, Y., T. Matsuzaki, T. Suzuki, T. Aoki, H. Hagiwara, M. Kuwahara, S. Sasaki, and K. Takata. 2004. Aquaporin-2 is retrieved to the apical storage compartment via early endosomes and phosphatidylinositol 3-kinase-dependent pathway. *Endocrinology.* 145:4375–4383.

Tesar, D.B., N.E. Tiangco, and P.J. Bjorkman. 2006. Ligand valency affects transcytosis, recycling and intracellular trafficking mediated by the neonatal Fc receptor. *Traffic.* 7:1127–1142.

Tesar, D.B., E.J. Cheung, and P.J. Bjorkman. 2008. The chicken yolk sac IgY receptor, a mammalian mannose receptor family member, transcytoses IgY across polarized epithelial cells. *Mol. Biol. Cell.* 19:1587–1593.

Thompson, A., R. Nessler, D. Wisco, E. Anderson, B. Winckler, and D. Sheff. 2007. Recycling endosomes of polarized epithelial cells actively sort apical and basolateral cargos into separate subdomains. *Mol. Biol. Cell.* 18:2687–2697.

Ullrich, O., S. Reinsch, S. Urbe, M. Zerial, and R.G. Parton. 1996. Rab11 regulates recycling through the pericentriolar recycling endosome. *J. Cell Biol.* 135:913–924.

van Ijzendoorn, S.C. 2006. Recycling endosomes. *J. Cell Sci.* 119:1679–1681.

van Ijzendoorn, S.C.D., and D. Hoekstra. 1999. The subapical compartment: a novel sorting center? *Trends Cell Biol.* 9:144–149.

Wakabayashi, Y., P. Dutt, J. Lippincott-Schwartz, and I.M. Arias. 2005. Rab11a and myosin Vb are required for bile canalicular formation in WIF-B9 cells. *Proc. Natl. Acad. Sci. USA.* 102:15087–15092.

Wang, E., P.S. Brown, B. Aroeti, S.J. Chapin, K.E. Mostov, and K.W. Dunn. 2000a. Apical and basolateral endocytic pathways of MDCK cells meet in acidic common endosomes distinct from a nearly-neutral apical recycling endosome. *Traffic.* 1:480–493.

Wang, X., R. Kumar, J. Navarre, J.E. Casanova, and J.R. Goldenring. 2000b. Regulation of vesicle trafficking in madin-darby canine kidney cells by Rab11a and Rab25. *J. Biol. Chem.* 275:29138–29146.

Wani, M.A., L.D. Haynes, J. Kim, C.L. Bronson, C. Chaudhury, S. Mohanty, T.A. Waldmann, J.M. Robinson, and C.L. Anderson. 2006. Familial hypercatabolic hypoproteinemia caused by deficiency of the neonatal Fc receptor, FcRn, due to a mutant β2-microglobulin gene. *Proc. Natl. Acad. Sci. USA.* 103:5084–5089.

Ward, E.S., C. Martinez, C. Vaccaro, J. Zhou, Q. Tang, and R.J. Ober. 2005. From sorting endosomes to exocytosis: association of Rab4 and Rab11 GTPases with the Fc receptor, FcRn, during recycling. *Mol. Biol. Cell.* 16:2028–2038.

Yoshida, M., S.M. Claypool, J.S. Wagner, E. Mizoguchi, A. Mizoguchi, D.C. Roopenian, W.I. Lencer, and R.S. Blumberg. 2004. Human neonatal fc receptor mediates transport of IgG into luminal secretions for delivery of antigens to mucosal dendritic cells. *Immunity.* 20:769–783.

Yoshida, M., K. Kobayashi, T.T. Kuo, L. Bry, J.N. Glickman, S.M. Claypool, A. Kaser, T. Nagaishi, D.E. Higgins, E. Mizoguchi, et al. 2006. Neonatal Fc receptor for IgG regulates mucosal immune responses to luminal bacteria. *J. Clin. Invest.* 116:2142–2151.

Zacchi, P., H. Stenmark, R.G. Parton, D. Orioli, F. Lim, A. Giner, I. Mellman, M. Zerial, and C. Murphy. 1998. Rab17 regulates membrane trafficking through apical recycling endosomes in polarized epithelial cells. *J. Cell Biol.* 140:1039–1053.